

CORROSION RESISTANCE OF AMORPHOUS Ni-Mo-P-ZrO₂ ELECTRODEPOSITED COATING

Yu Helong, Xu Yi, Shi Peijing, Wang Hongmei, Xu Binshi

National Key Laboratory for Remanufacturing, Beijing 100072, China

Zhao Chunfeng

Department of Training Management, Bengbu Tank Institute, Bengbu 233013, China

Ma Jie

Department of Chemistry, Capital Normal University, Beijing 100037, China

Abstract

The amorphous Ni-Mo-P-ZrO₂ nanocomposite coatings were prepared by electrodeposition in a Ni-Mo-P plating bath containing 20g/L ZrO₂ nanoparticles to be co-deposited. The influence of heat treatment temperature on the phase structure and microhardness of Ni-Mo-P coatings and the composite coatings were investigated. Potentiodynamic polarization technique was carried out to determine the corrosion behaviors of the two coatings in 5 wt% NaCl solution at room temperature. Results demonstrate that the as-deposited Ni-Mo-P-ZrO₂ coating has an amorphous structure. Its degree of crystallization was lower than that of Ni-Mo-P coating at the same heat treatment temperature. The introducing of ZrO₂ nanoparticles significantly improves the microhardness, thermal stability and corrosion resistance of the nanocomposite coating.

Keywords: Electrodeposition; Ni-Mo-P coating; ZrO₂ nanoparticles; composite coating; Corrosion resistance

1. Introduction

Ni-P alloy coatings, prepared by electrodeposition or electroless method, have been widely applied in many industries due to their good corrosion resistance and high hardness (hence high wear resistance). It is thus of interest to assess some ternary nickel-based alloys such as Ni-Cu-P^[1-4], Ni-W-P^[5-7], Ni-Mo-P^[8], Ni-Fe-P^[9-11], Ni-Co-P^[12], Ni-Sn-P^[13], Ni-Zn-P^[14], and Ni-Re-P^[15,16], which have also been developed to further improve these properties of binary systems by adding the second metal salts to nickel solution for meeting some special demands.

Recently, a large number of literatures reported nanoparticles such as SiC^[17, 18], ZrO₂^[19], Al₂O₃^[20], TiO₂^[21], SiO₂^[22], PTFE^[23, 24] and CeO₂^[22], which were

added to the plating bath and could be co-deposited with metal or alloy to form composite coatings. As shown in the researches, introduction of the second phase particles into the coatings enhanced their service properties further.

Among the possible metals, molybdenum appears to be of significant importance due to its high hardness, excellent corrosion resistance, high melting point, and relatively low cost^[25]. Ni-Mo-P amorphous alloy was developed as one of the surface treatments to replace hard chromium coating for its excellent properties, and the process was according to the consideration of environmental protection^[26]. Among the insoluble particulates used for reinforcement, ZrO₂ is frequently studied and applied for its good properties such as high hardness, good oxidation resistance and excellent good chemical stability^[27-30]. However, little attention has been paid to the incorporation of ZrO₂ nano-particulates in Ni-Mo-P matrix. So far few works have been reported on the preparation and mechanical and corrosion resistance properties of ZrO₂ nano-particulates co-deposited with Ni-Mo-P matrix by electrodeposition method.

The main purpose of this research was to co-deposit ZrO₂ nanoparticles into the amorphous Ni-Mo-P matrix by electrodeposition method in order to further improve the thermal stability and corrosion resistance. The influence of heat treatment temperature on the microhardness and phase structures of the nanocomposite coating was also reported.

2. Experimental

The cathode (substrate) and anode matrix were AISI 1045 steel disc (Φ25.6×6 mm) and pure nickel sheet (99.99%, 10×10×1.0 mm), respectively. Table 1 gives the operating conditions and chemical compositions of

the plating bath. Thiourea and dodecyl-mahogany soap were used as stabilizing agent and wetting agent, respectively. The High Energy Mechanical and Chemistry method (HEMC, a patent method) was utilized to achieve good dispersion and suspension stabilities of ZrO_2 nanoparticles in the electrodepositing solution. PMAA- NH_4 with an average molecular weight of 8000 was used as the modifying agent to produce an organic coating layer. After the process flow of electrodepositing, such as cleaning, activating, pre-electrolysis and plating, Ni-Mo-P and Ni-Mo-P- ZrO_2 coatings were prepared on 1045 steel substrate.

	Concentration (mol/L)
Plating bath composition	
$Ni_2SO_4 \cdot 6H_2O$	0.15
$(NH_4)_6Mo_7O_{24} \cdot 4H_2O$	Mo: 0.1
$NaH_2PO_2 \cdot H_2O$	0.2
$Na_3C_6H_5O_7 \cdot 2H_2O$	0.3
NaCl	0.30
Ammonia liquor (ml/L)	25
Operating conditions	
pH	9.0
J ($A \cdot dm^2$)	16
Duration (min)	120
Temperature ($^{\circ}C$)	25 ± 1

Table 1: Operating conditions and chemical compositions of the plating bath.

Heat treatment tests were carried out on a muffle furnace under the temperature of 200, 400 and 600 $^{\circ}C$. The rising rate of temperature and the holding time were 0.5 $^{\circ}C/s$ and 3 hours, respectively. The microhardness test was implanted in the microhardness tester (HX-1000). During the test, the load was fixed at 25 g and the loading time was fixed at 15 s.

The electrochemical tests were conducted in aerated 5 wt% NaCl solution at ambient temperature of about 22 $^{\circ}C$. A three-electrode cell configuration was employed for the measurements. A saturated calomel electrode (SCE) was used as the reference, the prepared coatings as the working electrode, and a platinum sheet as the counter electrode. Potentiodynamic polarization was carried out using a PARC 273 potentiostat manufactured by EG&G Company USA. Polarization scale ranged of ± 400 mV with respect to the corrosion potential. The current

was recorded as the potential increased at a rate of 0.166 mV/s. Data were automatically collected and analyzed with CORRVIEW software.

3. Results and discussions

3.1 Characterizations of the coatings

Figure 1(a) and (b) demonstrate the typical morphologies of Ni-Mo-P coating and Ni-Mo-P- ZrO_2 coating, respectively. It is seen that the two coatings both show granular surfaces. The grains of the composite coating were fine and the surface was close and smooth, bonding was compact and there were hardly flaws compared with Ni-Mo-P coating. It could be concluded that the nano- ZrO_2 grains can refine remarkably the structure of the electrodeposition coating.

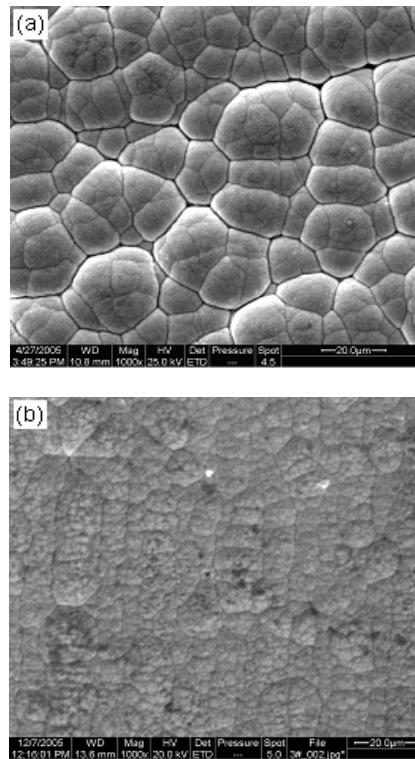


Fig.1 Morphologies of Ni-Mo-P and Ni-Mo-P- ZrO_2 coatings. (a) Ni-Mo-P coating. (b) Ni-Mo-P- ZrO_2 coating.

Figure 2(a) and (b) show the XRD results of Ni-Mo-P coating and Ni-MO-P- ZrO_2 composite coating that treated under different temperatures, respectively. It is obvious that under the as-deposited condition, the two XRD patterns both show only one broad peak at $2\theta=46.6^{\circ}$, showing the as-deposited coatings have an amorphous structure. Moreover, the additional peaks originating from ZrO_2 at $2\theta=28^{\circ}$ and 32° can be noticed in the X-ray patterns of the as-deposited Ni-Mo-P- ZrO_2

coating. The result demonstrates that the incorporation of ZrO_2 nanoparticles into the electrodeposited Ni-Mo-P matrix does not affect its structure. The XRD patterns of the coatings treated at $200^\circ C$ become sharp but still halo. When annealed at $400^\circ C$, the XRD pattern changes from halo to many sharp peaks for Ni-Mo-P coating, indicating the coating has crystallized and a large number of Ni_3P phase has appeared. When the temperature reaches $600^\circ C$, the crystallization of the amorphous Ni-Mo-P alloy completed and a large number of NiO phase appeared. For the Ni-Mo-P- ZrO_2 coating, it also crystallized at $400^\circ C$, but the degree of crystallization and the peak intensity of Ni_3P and NiO phase were lower than those of Ni-Mo-P-coating. The diffraction pattern of the composite coating annealed at $600^\circ C$ demonstrated the degree of crystallization increased but not a completed crystallized structure. It is believed that the dispersion-distributed ZrO_2 nanoparticles have good resistance to elevated temperatures, which can restrain the oxidation of the composite coatings and prevent the growth of crystal grain and recrystallization. Thus, the degree of crystallization and oxidation of Ni-Mo-P- ZrO_2 coating was decreased.

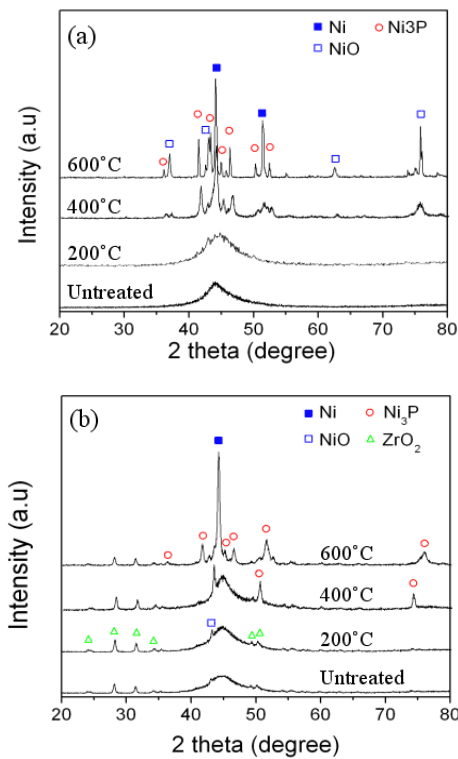


Fig. 2 XRD patterns of the coatings heat-treated at different temperatures. (a) Ni-Mo-P coating. (b) Ni-Mo-P- ZrO_2 coatings.

Figure 3 shows the variation curve of microhardness with temperature between the nanocomposite coating and Ni-Mo-P coating. It can be seen that the hardness, especially the high temperature hardness of the former was more superior to the latter. The hardness of Ni-Mo-P coating decreased rapidly once the temperature was over $400^\circ C$, whereas the hardness of Ni-Mo-P- ZrO_2 coating kept stable in spite of the temperature was up to $600^\circ C$. Further more, it could also hold a fairly good hardness at $700^\circ C$. So it is believed that the Ni-Mo-P- ZrO_2 composite coatings could play a permanent wear-resistance role at high temperature.

The nano-scale ZrO_2 grains were the high-hardness ceramic grains. When they were dispersed evenly in Ni-Mo-P matrix, the coating was strengthened by dispersion intensification, and its structure was improved. Thus, the microhardness of as-deposited Ni-Mo-P- ZrO_2 coating was superior to as-deposited Ni-Mo-P coating. According to the XRD results shown in Fig.4, the two coatings have not crystallized when annealed at $200^\circ C$. In this case, the increase of microhardness of the coatings could be explained by the structure relaxation and rearrangement of atoms in the alloy coatings. With the increasing of annealing temperature, the structure of the alloy coatings transferred from amorphous state to crystalline state. In this case, the microhardness of the alloy coatings depended on two factors. On the one hand, the precipitated phase of NiP intermetallic compound increased the drag in the dislocation movement of plastic deformation of the alloy coatings, as increased hardness of the coatings. On the other hand, with the growth of Ni-Mo-P solid solution at high temperature, the NiP compound aggregated and became coarsening, which caused reduction of its dispersity and the decrease of hardness. As a result of the two factors, the microhardness of the alloy coatings increased first and then decreased with temperature increasing.

Moreover, it is noted that the maximum microhardness of the annealed Ni-Mo-P- ZrO_2 coatings can be obtained at approximately $600^\circ C$, whereas it is about $400^\circ C$ for Ni-Mo-P coatings. That means we can improve the microhardness of the nanocomposite coating by annealing it at higher temperature. Two possible mechanisms resulted from the ZrO_2 nanoparticles resulted in the high temperature microhardness increase of the Ni-Mo-P- ZrO_2 coatings. (1) Fine crystal

intensification. The ZrO_2 nanoparticles blocked the grain growth of the precipitated phase, as a result, the crystal grains were smaller and the crystal boundary was more. (2) Dislocation intensification. Due to the uniform distribution of ZrO_2 nanoparticles in the coatings, it is possible that a large number of nanoparticles situated in the crystal boundary, as a result a high-density group of dislocation obstruction could be formed and block the dislocation slippage.

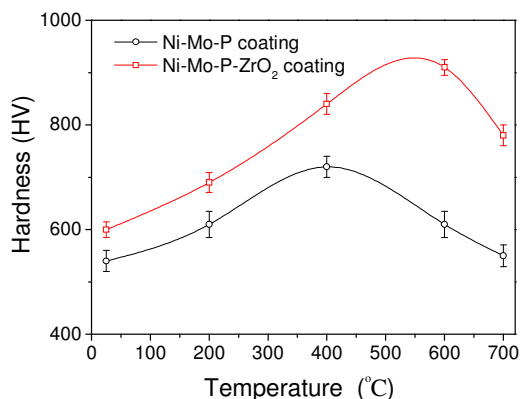


Fig.3 Variation of microhardness of Ni-Mo-P coating and Ni-Mo-P-ZrO₂ coating with temperature.

3.2. Corrosion resistance property

The corrosion behaviors of 1045 steel, Ni-Mo-P and Ni-Mo-P-ZrO₂ coatings in 5 wt% NaCl solution were studied as shown in Fig.4. The fitting results of polarization curves are listed in Table 2. It needed to explain that the thickness of Ni-Mo-P and Ni-Mo-P-ZrO₂ coatings was almost the same, 70-80 μm . It was found that the shapes of potentiodynamic curves were similar for both coatings: active reaction dominating the anodic sides and oxygen reduction dominating the cathodic sides. It implied that the anodic dissolution reaction of Ni-Mo-P-ZrO₂ coatings was restrained, which could be correlated to the reduction of the active surface due to the presence of inert ZrO_2 nanoparticles. Compared with 1045 steel substrate, the corrosion potential (E_{corr}) of Ni-Mo-P coating and Ni-Mo-P-ZrO₂ coating positively shifted about 195 mV and 210 mV, respectively, and the corrosion current density (i_{corr}) lowered nearly by 84% and 97%, respectively. Thus, the two coatings can provide adequate protection to the 1045steel in NaCl corrosive mediums. Furthermore, the result indicated that the corrosion resistance of Ni-Mo-P-ZrO₂ coatings was superior to Ni-Mo-P coatings.

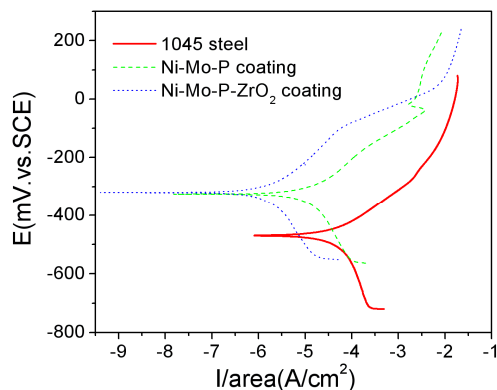


Fig. 4 Polarization curves of 1045 steel and the coatings in 5%NaCl solution.

The better electrochemical performance of the Ni-Mo-P-ZrO₂ nanocomposite coatings may be attributed to the reduction in the defect size of the nanocomposite coatings by the incorporation of ZrO_2 nanoparticles, which is helpful to segregate the corrosive medium. Besides, the ZrO_2 nanoparticles, which act as inert physical barriers to the initiation and development of defect corrosion, were embedded in Ni-Mo-P matrix and filled in crevices, gaps and pits. The deposition of the ZrO_2 nanoparticles in the composite coatings can also help to prevent the corrosive pits from growing up, and the incorporation of nano-particulates contributes to accelerate the passivation process of the metal matrix as well. Subsequently, the corrosion resistance of the nanocomposite coatings was improved.

	E_{corr} (mV)	i_{corr} ($\mu\text{A}/\text{cm}^2$)	E_a (mV)	E_c (mV)
1045 steel	-523.10	78.59	128.5	488.8
Ni-Mo-P	-327.98	12.16	132.9	524.2
Ni-Mo-P-ZrO ₂	-313.50	2.515	169.1	306.2

Table 2 Electrochemical parameters of 1045steel and coatings in 5%NaCl solution.

4. Conclusions

- (1) It is feasible to prepare amorphous Ni-Mo-P-ZrO₂ nanocomposite coating by properly incorporating the nano-particulates to be co-deposited in the Ni-Mo-P plating bath.
- (2) The dispersion-distributed ZrO_2 nanoparticles, with good resistance to elevated temperatures, restrained the oxidation of the composite coatings and prevent the crystal grain growth and recrystallization. Therefore, the degree of crystallization of Ni-Mo-P-ZrO₂ was decreased and its thermal stability was superior to Ni-Mo-P.

(3) The corrosion resistance of Ni-Mo-P-ZrO₂ composite coatings was enhanced due to the better adhesion, more compact structure, and lower porosity caused by the introduction of ZrO₂ nanoparticles. The composite coating was partly separated from the corrosion medium by ZrO₂ particulates, which present lower chemical activity.

Acknowledgement

This research was supported by the Key Basic Research & Development Program of China (2007CB607601) and National Natural Science Foundation of China (50735006, 50805146).

References

- [1] H. S. Yu, S. F. Luo, Y. R. Wang, *Surf. Coat. Technol.* 148 (2001) 143.
- [2] Y. Liu, Q. Zhao, *Appl. Surf. Sci.* 228 (2004) 57.
- [3] K. L. Lin, Y. L. Chang, C. C. Huang, F. I. Li, J. C. Hsu, *Appl. Surf. Sci.* 181 (2001) 166.
- [4] J. N. Balaraju, K. S. Rajam, *Surf. Coat. Technol.* 195 (2005) 154.
- [5] S. K. Tien, J. G. Duh, Y. I. Chen, *Surf. Coat. Technol.* 177–178 (2004) 532.
- [6] J. N. Balaraju, C. Anandan, K. S. Rajam, *Surf. Coat. Technol.* 200 (2006) 3675.
- [7] J. N. Balaraju, S. M. Jahan, C. Anandan, K. S. Rajam, *Surf. Coat. Technol.* 200 (2006) 4885.
- [8] G. J. Lu, G. Zangari, *Electrochem. Acta.* 47 (2002) 2969.
- [9] L. L. Wang, L. H. Zhao, G. F. Huang, X. J. Yuan, B. W. Zhang, J. Y. Zhang, *Surf. Coat. Technol.* 126 (2000) 272.
- [10] S. L. Wang, *Surf. Coat. Technol.* 186 (2004) 372.
- [11] C. H. Gao, *Trans. Nonferrous Met. Soc. China* 16(2006) 1325.
- [12] M. M. Younan, I. H. M. Aly, M. T. Nageeb, *J. Appl. Electrochem.* 32 (2002) 439.
- [13] B. W. Zhang, H. W. Xie, *Mater. Sci. Eng. A* 281 (2000) 286.
- [14] M. Bouanani, F. Cherkaoui, R. Fratesi, G. Roventi, G. Barucca, *J. Appl. Electrochem.* 29 (1999) 637.
- [15] D. Mencer, *J. Alloys Compd.* 306 (2000) 158.
- [16] E. Valova, S. Armanyanov, A. Franquet, A. Hubin, O. Steenhaut, J. L. Delplanche, J. Vereecken, *J. Appl. Electrochem.* 31 (2001) 1367.
- [17] Y. W. Yao, S. W. Yao, L. Zhang, H. Z. Wang, *Materials Letters.* 61 (2007) 67–70.
- [18] M. R. Vaezi, S. K. Sadrezaad, L. Nikzad, *Colloids and Surfaces A: Physicochem. Eng. Aspects.* 315 (2008) 176.
- [19] B. Jiang, B. S. Xu, S. Y. Dong, Y. Yi, P. D. Ding, *Surf. Coat. Technol.* 202 (2007) 447.
- [20] Z. Zeng, J. Zhang, *Surf. Coat. Technol.* (2007), doi:10.1016/j.surfcoat.2007.10.008.
- [21] Z. H. Zhao, Y. Sakagami, T. Osaka, *Chem. Lett.* 9 (1997) 909.
- [22] R. D. Xu, J. L. Wang, L. F. He, Z. C. Guo, *Surf. Coat. Technol.* 202 (2008) 1574.
- [23] Z. C. Guo, R. D. Xu, X. Y. Zhu, *Surf. Coat. Technol.* 187 (2004) 141.
- [24] Q. Zhao, Y. Liu, C. Wang, *Appl. Surf. Sci.* 252 (2005) 1620.
- [25] J. Okado, M. Shima, I. R. McColl, R. B. Waterhouse, T. Hasegawa, M. Kasaya, *Wear* 225–229 (1999), 749–757.
- [26] G. Lu, P. Evans, G. Zangari, *J. Electrochem. Soc.* 150 (2003) A551.
- [27] F. Y. Hou, W. Wang, H. T. Guo, *Appl. Surf. Sci.* 252 (2006) 3812.
- [28] W. Wang, F. Y. Hou, H. Wang, H. T. Guo, *Scripta Materialia.* 53 (2005) 613.
- [29] Y. W. Song, D. Y. Shan, E. H. Han, *Electrochimica Acta.* 53 (2008) 2135–2143.
- [30] B. Szczygieł, A. Turkiewicz, J. Serafińczuk, *Surf. Coat. Technol.* 202 (2008) 1904.

*helong.yu@163.com; phone +86 10 66718580; fax: +86 10 66717144; National Key Laboratory for Remanufacturing, Academy of Armored Forces Engineering, No. 21 Dujiakan, Changxindian, 100072 Beijing, PR China.